

Elastic Gauge Fields in Weyl Semimetals

Alberto Cortijo,¹ Yago Ferreirós,¹ Karl Landsteiner,² and María A. H. Vozmediano¹

¹*Instituto de Ciencia de Materiales de Madrid, CSIC, Cantoblanco; 28049 Madrid, Spain.*

²*Instituto de Física Teórica UAM/CSIC, Nicolás Cabrera 13-15, Cantoblanco, 28049 Madrid, Spain*

(Dated: March 9, 2016)

We show that, as it happens in graphene, elastic deformations couple to the electronic degrees of freedom as pseudo gauge fields in Weyl semimetals. We derive the form of the elastic gauge fields in a tight-binding model hosting Weyl nodes and see that this vector electron-phonon coupling is chiral, providing an example of axial gauge fields in three dimensions. As an example of the new response functions that arise associated to these elastic gauge fields, we derive a non-zero phonon Hall viscosity for the neutral system at zero temperature. The axial nature of the fields provides a test of the chiral anomaly in high energy with three axial vector couplings.

PACS numbers:

Introduction.— The occurrence of Weyl fermions (massless Dirac fermions of definite chirality) in condensed matter has come always with unexpected phenomena and new physics. Although having a long tradition [1], the best examples so far arose in one spacial dimension (Luttinger liquids) [2] or in two (Graphene [3] and the surface of three dimensional topological insulators [4]). Charged massless fermions are particularly interesting in three dimensions: They do not have counterparts in particle physics and they experience the chiral anomaly [5–9] and its related physical responses.

The Dirac equation comes from the existence of band crossings, “Fermi points” in the dispersion relation and subsequent low energy expansion around them. Coming from a lattice, these Weyl fermions must always arise in pairs of opposite chirality – or helicity – according to the Nielsen-Ninomiya theorem [7]. Dirac semimetals [10] have the crossing points at the gamma point of the Brillouin zone and the contribution from the two opposite chiralities cancel the anomaly related responses. The importance of the so-called Weyl semimetals is that, as happens in graphene, the two chiral partners sit at non equivalent points in momentum space and the physics of anomalies is present in full glory. This is why the recent experimental discovery of Weyl semimetals (WSM) [11–15] is attracting so much excitement [16].

WSM have been named “the 3D graphene”. One of the most exotic and fruitful aspects of graphene has arisen from the demonstration that elastic lattice deformations couple to its electronic excitations in the form of fictitious gauge fields [17]. This fact, first deduced in a tight-binding model [18] was soon recognized to arise from very general symmetry considerations [19, 20]. The experimental observation of the predicted Landau levels associated to the elastic magnetic fields [21, 22], have given rise to a whole new field of research called “straintronics”.

In what follows we will show the presence of elastic gauge fields in WSM. We first make a microscopic deriva-

tion starting from a tight-binding description [18] and taking the continuum limit around the Weyl points. As a physical consequence, we will show the presence of an anomalous phonon Hall viscosity in the WSM with time reversal symmetry (\mathcal{T}) broken. Similar to the Hall conductivity, the Hall viscosity can be used to classify topologically non-trivial states of matter [23–28]. We will see that the elastic gauge fields provide a new mechanism for generating Hall viscosity not previously studied in the literature. Due the chiral nature of the coupling between Weyl fermions and elastic degrees of freedom, this new coupling provides an example of axial vector-fermion interaction with no analogue in high energy physics, and paves the way for studying the consequences of such couplings in a more general context.

Elastic gauge fields in a model for WSM.— To illustrate how emergent vector fields associated to elasticity appear in a WSM phase we can consider the following simple model of s-, and p-like electrons hopping in a cubic lattice and chirally coupled to an on-site constant vector field \mathbf{b} [29, 30]

$$H_0 = \sum_{i,j} c_i^\dagger \left(it\alpha_j - r\hat{\beta} \right) c_{i+j} + (m + 3r) \sum_i c_i^\dagger \hat{\beta} c_i + \sum_{i,l} b_l c_i^\dagger \alpha_l \gamma_5 c_i + h.c., \quad (1)$$

where i labels the position \mathbf{R}_i and j labels the six next nearest neighbors \mathbf{a}_j of length a in the cubic lattice. The matrices α_i and $\hat{\beta}$ are the standard Dirac matrices. In the unstrained situation we will set all the hopping terms t equal for simplicity. The parameters t , r , and m , represent, in a tight-binding description, the hopping matrix elements between s and p states, hopping between the same kind of states, and the difference of on-site energies between s and p states, respectively. The vector field \mathbf{b} breaks \mathcal{T} as well as the cubic lattice symmetry and thus the SO(3) rotational symmetry in the continuum description. Without loss of generality, we will choose

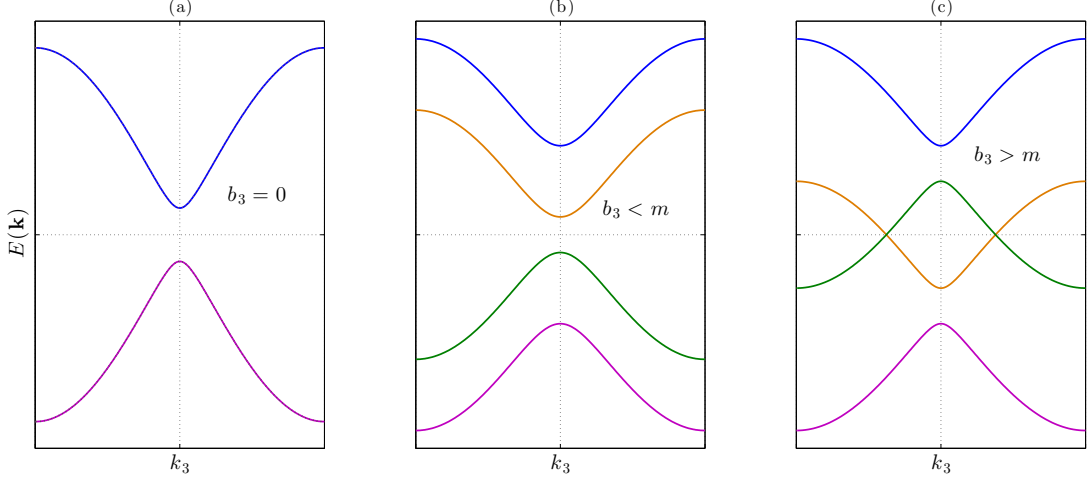


FIG. 1: (Color online.) Evolution of the band structure of the model given in eq. (1) as a function of the parameter b . For $b_3 = 0$ the spectrum consists in two pairs of degenerate bands due to time reversal symmetry, (a). When $0 < b_3 < m$ the band degeneracy breaks down and a high energy sector differentiates from a low energy sector, but the system is still gapfull, (b). When $b_3 > m$, the low energy bands cross each other at two definite points in the Brillouin zone. At sufficiently low energies, the system consists in two pairs of Weyl fermions with opposite chirality, (c).

the vector field \mathbf{b} to point along the OZ direction. The model of eq. (1) with $b_3 = 0$ is the standard model to exemplify the transition from a trivial to a topological insulating phase as a function of the parameters m and r . The region $0 > m > -2r$ corresponds to a topological insulating phase and the long wavelength limit around the Γ point ($\mathbf{k} = 0$) corresponds to an isotropic massive Dirac system. As it can be seen in Fig.(1) the WSM phase ap-

pears when $b_3 > m$. The spectrum of the Hamiltonian in eq.(1) consists of two bands crossing at two Fermi points in the BZ and two bands at higher and lower energies (Fig.(1,c)). Let us choose the following representation for the Dirac matrices: $\alpha_1 = \tau_0\sigma_1$, $\alpha_2 = \tau_0\sigma_2$, $\alpha_3 = \tau_1\sigma_3$, $\hat{\beta} = \tau_3\sigma_3$, $\gamma_5 = \tau_1\sigma_0$, so $\alpha_3\gamma_5 = \tau_0\sigma_3$. Fourier transforming (1) we obtain:

$$\mathcal{H}_0(\mathbf{k}) = \begin{pmatrix} t \sum_s \sigma_s \sin(k_s a) + (b_3 + m(\mathbf{k}))\sigma_3 & t \sin(k_3 a)\sigma_3 \\ t \sin(k_3 a)\sigma_3 & t \sum_s \sigma_s \sin(k_s a) + (b_3 - m(\mathbf{k}))\sigma_3 \end{pmatrix}, \quad (2)$$

with $s = (1, 2)$, and $m(\mathbf{k}) = m + 3r - r \sum_j \cos(k_j a)$. The four-component wavefunction can be written in two-component blocks $(\phi_{\mathbf{k}}, \psi_{\mathbf{k}})$. For energies $E \ll m + b_3$ we can write $\phi_{\mathbf{k}} \simeq -\frac{vk_3}{m+b_3}\psi_{\mathbf{k}}$. Projecting out the high energy sector represented by $\phi_{\mathbf{k}}$ and expanding around the $\mathbf{k} = 0$ point, we find the following effective two-band model in the continuum ($v = ta$):

$$H_{eff} = \sum_{\mathbf{k}} \psi_{\mathbf{k}}^\dagger \left(v\boldsymbol{\sigma}_\perp \cdot \mathbf{k}_\perp + \frac{1}{m+b_3}(b_3^2 - m^2 - v^2 k_3^2)\sigma_3 \right) \psi_{\mathbf{k}}. \quad (3)$$

The existence of Weyl points $\boldsymbol{\lambda}$ is met when for $k_1 = k_2 = 0$, the equation $b_3^2 - m^2 - v^2 k_3^2 = 0$ has real solutions. In this case, the two Weyl points are located at $\boldsymbol{\lambda}_\pm = (0, 0, \pm\sqrt{\frac{b_3^2 - m^2}{v^2}})$. Expanding now around these two points $\mathbf{k} \simeq \boldsymbol{\lambda}_\pm + \delta\mathbf{k}$, the low energy effective Hamiltonian takes the form of two massless three dimensional Dirac fermions ψ_\pm separated by the vector $\boldsymbol{\lambda}_+ - \boldsymbol{\lambda}_-$ in

momentum space:

$$H_W = \sum_{\delta\mathbf{k}} \psi_{\pm, \delta\mathbf{k}}^\dagger (v\boldsymbol{\sigma} \cdot \delta\mathbf{k}_\perp \mp v_3 \delta k_3 \sigma_3) \psi_{\pm, \delta\mathbf{k}}, \quad (4)$$

with $v_3 = 2v\sqrt{\frac{b_3 - m}{b_3 + m}}$.

Now we will apply strain to the original tight binding Hamiltonian and find the modifications it induces in the

low energy Hamiltonian (4). The strain tensor u_{ij} enters in the tight binding approach through the change of the hopping parameters t when the lattice is distorted. In the model of eq. (1), there are two types of corrections to t . One, similar to that arising in graphene [17], is due to the change in the bond length. It is isotropic and exists for all orbitals:

$$r \rightarrow r_j \simeq r(1 - \beta u_{jj}), \quad (5)$$

where β is the Grüneisen parameter of the model. The second contribution affects the hopping between different orbitals and is associated to a rotation with respect to the reference frames of neighbouring atoms as described in [30]. Following this reference, the changes for t_j are:

$$t\alpha_j \rightarrow t(1 - \beta u_{jj})\alpha_j + t\beta \sum_{j' \neq j} u_{jj'}\alpha_{j'}. \quad (6)$$

Inserting these modifications in the original Hamiltonian (1), we can define the strained Hamiltonian as the sum of the original Hamiltonian H_0 and the strain dependent part $H[u_{ij}]$. Projecting out the high energy sector and expanding around the two nodal points λ_{\pm} , the strain dependent Hamiltonian part takes the form

$$H_{eff}^W[u]_{\pm} = \pm\beta\sqrt{b_3^2 - m^2} \sum_{\mathbf{k}, s=1,2} u_{3s}\psi_{\pm, \mathbf{k}}^{\pm} \sigma_s \psi_{\pm, \mathbf{k}} + \beta \sum_{\mathbf{k}} \left(2(b_3 - m)u_{33} - r \sum_j u_{jj} \right) \psi_{\pm, \mathbf{k}}^{\pm} \sigma_3 \psi_{\pm, \mathbf{k}}. \quad (7)$$

We have found that, around the two nodal points, strain couples to the low energy electronic sector as a vector field:

$$\begin{aligned} A_1^{el} &= \beta\sqrt{b_3^2 - m^2}u_{31}, \\ A_2^{el} &= \beta\sqrt{b_3^2 - m^2}u_{32}, \\ A_3^{el} &= 2\beta(b_3 - m)u_{33} - \beta r \sum_j u_{jj}. \end{aligned} \quad (8)$$

This is the first main result of this Letter.

The low energy effective action in the continuum limit around the Weyl nodes (λ_{\pm}) is thus given by

$$H_W = \sum_{\delta\mathbf{k}} \psi_{\pm, \delta\mathbf{k}}^{\pm} \left(\boldsymbol{\sigma}(v\delta\mathbf{k}_{\perp} \pm \mathbf{A}_{\perp}^{el}) \mp (v_3\delta k_3 \pm A_3^{el})\sigma_3 \right) \psi_{\pm, \delta\mathbf{k}}. \quad (9)$$

Similarly to what happens in graphene or other two dimensional systems, strain couples to electrons as a chiral vector field i. e. it couples with opposite signs to the electronic excitations around the two Weyl nodes. The specific form of (8) is due to the choice of the vector \mathbf{b} pointing along the OZ axis.

Hall viscosity. – As a physical consequence of the presence of the elastic gauge fields, we will next show that WSM

have an intrinsic Hall viscosity. In visco-elastic systems the viscosity tensor is defined as the transport coefficient relating the stress tensor τ_{ij} and the *time derivative* of the strain tensor u_{rs} , $\tau_{ij} = \eta_{ijrs}\dot{u}_{rs}$. The antisymmetric part of η_{ijrs} is a dissipationless coefficient allowed only when \mathcal{T} is broken. In three dimensions rotational symmetry must also be broken to get a nonvanishing Hall viscosity. For axially symmetric systems with broken \mathcal{T} there are two independent components of the Hall viscosity tensor that can be chosen η_{3231} and η_{1112} [23]. The Hall viscosity was first defined as an intrinsic property of the quantum fluid. When a topologically non-trivial electronic fluid is coupled to the crystal environment it will induce a Hall viscosity term in the elastic free energy of phonons [31]. The electronic contribution to the field theory for the elastic degrees of freedom can be obtained by integrating out the electronic fields in (9). The effective action will contain the following term (in units $\hbar = 1$):

$$\begin{aligned} \Gamma_H[u] &= \frac{1}{48\pi^2} \int d^4x \epsilon^{\mu\nu\rho\sigma} \lambda_{\mu} A_{\nu}^{el} \partial_{\rho} A_{\sigma}^{el} = \\ &= \frac{\beta^2}{48\pi^2 a^3} \left(\frac{b_3^2 - m^2}{t^2} \right)^{\frac{3}{2}} \int d^4x (u_{31}\dot{u}_{32} - u_{32}\dot{u}_{31}) \end{aligned} \quad (10)$$

From this expression, we can easily read the coefficient $\eta_H = \eta_{3231}$ of Hall viscosity coming from the presence of the elastic gauge fields:

$$\eta_H = \frac{\beta^2}{24\pi^2} \frac{1}{a^3} \left(\frac{b_3^2 - m^2}{t^2} \right)^{\frac{3}{2}}. \quad (11)$$

This is the second main result of this letter: In the simple model considered, both \mathcal{T} and rotational invariance are broken by the presence of the constant vector \mathbf{b} giving rise to a Hall viscosity through the elastic vector fields. This response is rooted on the topological nature of the material and is universal in the sense that it is directly related to the Hall conductivity. For a general 3D Weyl semimetal breaking time reversal symmetry, the anomalous hall effect is characterized by a momentum space vector called the Chern vector. In our model, this is the vector λ_{μ} separating the two Weyl nodes in momentum space. The anomalous hall conductivity is given by the expression: $\sigma_{ij} = \frac{e^2}{2\pi c} \epsilon_{ijk} \lambda_k$, coming from a 3D Chern Simons term of the form

$$S_{CS} \sim \nu_H \int d^4x \lambda_i \epsilon^{ijkl} A_j \partial_k A_l, \quad (12)$$

where ν_H is the 3D Hall conductivity. It is easy to recognize the first term of eq. (10) as the Chern Simons term associated to the elastic gauge fields. As a rule, what we have shown is that, any Hall system supporting elastic gauge fields will automatically present a Hall viscosity response.

Discussion. – As a proof of concept, we have shown that WSMs couple to elasticity through chiral vector fields by

using a minimal tight-binding lattice model. This fact is not tied to the breakdown of time reversal symmetry, although we have used a model where the Weyl points appear by breaking \mathcal{T} (a system with broken time reversal symmetry has been reported in [15]). A necessary condition (albeit it might not be sufficient) for having such elastic gauge fields (technically, to have a vector representation of the elastic degrees of freedom at the Weyl point) is to have the Weyl points sitting at non-equivalent points of the Brillouin zone (what excludes the Γ point) [19]. The presence of Weyl points is compatible with \mathcal{T} if the pair of Weyl nodes are related by inversion symmetry \mathcal{I} [32]. This implies that these elastic gauge fields will appear in most of the \mathcal{T} -invariant systems displaying Weyl nodes, implying the generality of this phenomenon.

As a direct consequence of this chiral vector coupling between elasticity and the electronic degrees of freedom, a new type of Hall viscosity arises in WSMs. In three dimensions Hall viscosity has been discussed in the literature associated to two instances only: The topological insulator phase with \mathcal{T} broken and a WSM system in the presence of torsion [30, 33]. The elastic gauge fields coupled to a topologically non-trivial system defines a third mechanism that will act on topologically non trivial crystals supporting elastic vector fields.

Several aspects of the viscoelastic response of lattice topological crystals have been recently analyzed in [30]. Our new contribution to the Hall viscosity, although not explicitly discussed, could certainly have been worked out as a part of their general analysis. The examples chosen there having the Weyl nodes at the gamma point prevented them from finding the elastic gauge fields. The coupling giving rise to the Hall viscosity in that reference is linear in momentum and corresponds to the standard phonon viscosity found in the hydrodynamic approach [24]. In contrast, the elastic gauge field term described in our work couples directly to the fermionic current and is of lowest order in a derivative expansion.

Another important aspect of the present analysis arises in the connection of the new term with the chiral anomaly. As we discussed, the elastic vector fields are chiral in the sense that they couple with opposite signs to the two chiralities. Moreover, the field λ_μ is also an axial field what implies that the coefficient in eq. (10) is associated to the triangular graph with three axial vertices (AAA). This triangular graph has an additional symmetry factor of 1/3 compared to the usual one (one axial and two vector vertices AVV). We would like to emphasize that this gives rise to the exciting possibility to test the AAA anomaly in a condensed matter context. In contrast it is generally believed that this type of anomaly does not lead to physical consequences in high energy physics [34].

The existence of elastic gauge fields in WSMs extends the field of "straintronics" to three-dimensional materials and paves the path for the study of a plethora of

emergent phenomena. Notice that Weyl points are not an exclusive property of the dispersion relation of electronic systems. They have also been described in three dimensional photonic systems [35, 36] what allows to envisage the extension of "straintronics" to photonic media by controlling the Weyl nodes with deformations through these elastic gauge fields.

Acknowledgments. – We thank Carlos Hoyos for enlightening discussions on the Hall viscosity and Juan Mañes for comments on the elastic gauge fields. Special thanks go also to José Silva-Guillén for help with the figures. This research was supported in part by the Spanish MEC grants FIS2011-23713, PIB2010BZ-00512, the European Union structural funds and the Comunidad de Madrid MAD2D-CM Program (S2013/MIT-3007), by the National Science Foundation under Grant No. NSF PHY11-25915, and by the European Union Seventh Framework Programme under grant agreement no. 604391 Graphene Flagship, FPA2012-32828 and by the Centro de Excelencia Severo Ochoa Programme under grant SEV-2012-0249.

-
- [1] Volovik, G. E. *The universe in a helium droplet* (Clarendon Press, Oxford, 2003).
 - [2] Giamarchi, T. *Quantum Physics in One Dimension* (University Press, Oxford, 2004).
 - [3] Castro Neto, A. H., Guinea, F., Peres, N. M. R., Novoselov, K. S. & Geim, A. K. The electronic properties of graphene. *Rev. Mod. Phys.* **81**, 109–162 (2009).
 - [4] Qi, X. & Zhang, S. Topological insulators and superconductors. *Rev. Mod. Phys.* **83**, 1057 (2011).
 - [5] Adler, S. L. Axial-vector vertex in spinor electrodynamics. *Phys. Rev.* **177**, 2426–2438 (1969).
 - [6] Bell, J. S. & Jackiw, R. A pcac puzzle: $\pi_0 \rightarrow \gamma\gamma$ in the σ model. *Nuovo Cimento A* **60**, 47 (1969).
 - [7] Nielsen, H. B. & Ninomiya, M. Absence of neutrinos on a lattice: (i). proof by homotopy theory. *Nuc. Phys. B* **185**, 20–40 (1981).
 - [8] Grushin, A. G. Consequences of a condensed matter realization of lorentz-violating qed in weyl semi-metals. *Phys. Rev. D* **86**, 045001 (2012).
 - [9] Goswami, P. & Tewari, S. Axionic field theory of (3+1)-dimensional weyl semimetals. *Phys. Rev. B* **88**, 245107 (2013).
 - [10] Liu, Z. K. *et al.* A stable three-dimensional topological dirac semimetal cd_3as_2 . *Nat. Mater.* **13**, 677–681 (2014).
 - [11] Huang, S.-M. *et al.* A weyl fermion semimetal with surface fermi arcs in the transition metal monopnictide TaAs class. *Nat Commun* **6** (2015).
 - [12] Xu, S.-Y. *et al.* Discovery of a weyl fermion semimetal and topological fermi arcs. *Science* (2015). arXiv:1502.03807.
 - [13] Xu, S. Y. *et al.* Discovery of a weyl fermion state with fermi arcs in niobium arsenide. *Nature Physics* (2015). arXiv:1502.01350.
 - [14] Huang, S. M. *et al.* A new type of weyl semimetal with quadratic double weyl fermions in Sr Si2.

- arXiv:1502.05868* (2015).
- [15] Borisenko, S. *et al.* Time-reversal symmetry breaking weyl state in Yb Mn Bi_2 . *arXiv:1507.04847* (2015).
- [16] Johnston, H. Weyl fermions are spotted at long last. *Physics World* **July 23** (2015).
- [17] Vozmediano, M. A. H., Katsnelson, M. I. & Guinea, F. Gauge fields in graphene. *Physics Reports* **493**, 109 (2010).
- [18] Suzuura, H. & Ando, T. Phonons and electron-phonon scattering in carbon nanotubes. *Phys. Rev. B* **65**, 235412 (2002).
- [19] J. L. Mañes. Symmetry-based approach to electron-phonon interactions in graphene. *Phys. Rev. B* **76**, 045430 (2007).
- [20] Mañes, J. L., de Juan, F., Sturla, M. & Vozmediano, M. A. H. Generalized effective hamiltonian for graphene under nonuniform strain. *Phys. Rev. B* **88**, 155405 (2013).
- [21] Guinea, F., Katsnelson, M. I. & Geim, A. G. Energy gaps, topological insulator state and zero-field quantum hall effect in graphene by engineering. *Nature Physics* **6**, 30 (2010).
- [22] Levy, N. *et al.* Strain-induced pseudomagnetic fields greater than 300 tesla in graphene nanobubbles. *Science* **329**, 544 (2010).
- [23] Avron, J. E., Seiler, R. & Zograf, P. G. Viscosity of quantum hall fluids. *Phys. Rev. Lett.* **75**, 697 (1995).
- [24] Tokatly, I. V. & Vignale, G. Lorentz shear modulus of a two-dimensional electron gas at high magnetic field. *Phys. Rev. B* **76**, 161305 (2007).
- [25] Read, N. Non-abelian adiabatic statistics and hall viscosity in quantum hall states and $p_x + ip_y$ paired superfluids. *Phys. Rev. B* **79**, 045308 (2009).
- [26] Hughes, T. L., Leigh, R. G. & Fradkin, E. Torsional response and dissipationless viscosity in topological insulators. *Phys. Rev. Lett.* **107**, 075502 (2013).
- [27] Bradlyn, B., Goldstein, M. & Read, N. Kubo formulas for viscosity: Hall viscosity, ward identities, and the relation with conductivity. *Phys. Rev. B* **86**, 245309 (2012).
- [28] Hoyos, C. & Son, D. T. Hall viscosity and electromagnetic response. *Phys. Rev. Lett.* **108**, 066805 (2012).
- [29] Vazifeh, M. M. & Franz, M. Electromagnetic response of weyl semimetals. *Phys. Rev. Lett.* **111**, 027201 (2013).
- [30] Shapourian, H., Hughes, T. L. & Ryu, S. The viscoelastic response of topological tight-binding models in 2d and 3d. *arXiv:1505.03868* (2015).
- [31] Barkeshli, M., Chung, S. B. & Qi, X. Dissipationless phonon hall viscosity. *Phys. Rev. B* **85**, 245107 (2012).
- [32] Mañes, J. L. Existence of bulk chiral fermions and crystal symmetry. *Phys. Rev. B* **85**, 155118 (2012).
- [33] Sun, L. & Wan, S. Chiral viscoelastic response in weyl semimetals. *Eur. Phys. Lett.* **108**, 37007 (2014).
- [34] Schwartz, M. D. *Quantum Field Theory and the Standard Model* (Cambridge University Press, 2013).
- [35] Lu, L., Fu, L., Joannopoulos, J. D. & Soljacic, M. Weyl points and line nodes in gyroid photonic crystals. *Nat. Photon.* **7**, 294–299 (2013).
- [36] Lu, L. *et al.* Experimental observation of weyl points. *Science* **349**, 622–624 (2015). URL <http://www.sciencemag.org/content/349/6248/622.abstract>. <http://www.sciencemag.org/content/349/6248/622.full.pdf>.